Supporting Material

A physiologically based pharmacokinetic model for polyethylene glycol-coated gold nanoparticles of different sizes in adult mice

Zhoumeng Lin[1], Nancy A. Monteiro-Riviere[2], Jim E. Riviere[1,*]

[1]Institute of Computational Comparative Medicine (ICCM); and [2]Nanotechnology Innovation Center of Kansas State (NICKS), Department of Anatomy and Physiology, College of Veterinary Medicine, Kansas State University, Manhattan, KS 66506, USA

* **Corresponding author**: ICCM, College of Veterinary Medicine, Kansas State University, Manhattan, KS 66506. E-mail: jriviere@ksu.edu; phone: +1-785-532-3683; fax: +1-785-532-4953.

Contents

Page

1. Mathematical representation of the model

1.1. Intravenous injection

Intravenous dosing was described with a single rate of administration to the venous blood, as shown below:

$$Dose_{iv} = PDOSE_{iv} \times BW \quad \text{(S1)}$$

$$R_{iv} = Dose_{iv} / Time_{iv} \quad \text{(S2)}$$

where $Dose_{iv}$ [mg] is the amount of injected dose to the animal, $PDOSE_{iv}$ [mg/kg] is the intravenous injection dose, BW [kg] is the body weight of the animal, R_{iv} [mg/h] is the rate of intravenous injection, and $Time_{iv}$ [h] is the duration of the injection. It was assumed that intravenous injection of the total dose was completed within 0.005h (i.e., set $Time_{iv}$ = 0.005h [18 sec]) and the bioavailability was 100%.

1.2. Distribution

1.2.1. Kinetics of the nanoparticles in the plasma (or blood) compartment

As shown in Figure 1, the rate of changes in the amount of the nanoparticles (NPs) in the arterial sub-compartment is equal to the rate from the lungs minus the rate to the other organs, and the rate in the venous sub-compartment is identical to the rate from these other organs minus the rate to the lungs, as described below:

$$R_a = QC \times CV_{Lu} - QC \times C_a \quad \text{(S3)}$$

$$A_a = \text{Integ}(R_a, 0.0) \quad \text{(S4)}$$

$$C_a = A_a / V_a \quad \text{(S5)}$$

$$R_v = Q_L \times CV_L + Q_{BR} \times CV_{BR} + Q_K \times CV_K + Q_{rest} \times CV_{rest} + R_{iv} - QC \times C_v \quad \text{(S6)}$$

$$A_v = \text{Integ}(R_v, 0.0) \quad \text{(S7)}$$

$$C_v = A_v / V_v \quad \text{(S8)}$$

where R_a [mg/h] is the rate of changes in the amount of the NPs in the arterial blood, QC [L/h] is the cardiac output of the animal, CV_{Lu} [mg/L] is the concentration of the NPs in the venous blood of the lungs, C_a [mg/L (μg/g) or ng/g depending on the original experimental data] is the concentration of the NPs in the arterial blood (or plasma), A_a [mg] is the amount of the NPs in the arterial blood, V_a [L] is the volume of the arterial blood, R_v [mg/h] is the rate of changes in the amount of the NPs in the venous blood, Q_L [L/h] is the blood flow to the liver, CV_L [mg/L] is the concentration of the NPs in the venous blood of the liver, Q_{BR} [L/h] is the blood flow to the brain, CV_{BR} [mg/L] is the concentration of the NPs in the venous blood of the brain, Q_K [L/h] is the blood flow to the kidneys, CV_K [mg/L] is the concentration of the NPs in the venous blood of the kidneys, Q_{rest} [L/h] is the blood flow to the rest of the body, CV_{rest} [mg/L] is the concentration of the NPs in the venous blood of the rest of body, R_{iv} [mg/h] is the rate of intravenous injection, C_v [mg/L] is the concentration of the NPs in the venous blood, A_v [mg] is the amount of the NPs in the venous blood, V_v [L] is the volume of the venous blood.

1.2.2. Kinetics of the nanoparticles in the organ compartment

For a membrane-limited model, the kinetics of the NPs in the capillary blood and the tissue of each organ should be described separately. For example, equations describing the kinetics of 100nm PEG-coated AuNPs in the sub-compartments of phagocytic cells (PCs), capillary blood, and tissue of each organ are shown below:

$$R_{up\_t} = K_{up\_t} \times A_{b\_t} \quad \text{(S9)}$$

$$R_{release\_t} = K_{release\_t} \times A_{pc\_t} \quad \text{(S10)}$$

$$R_{pc\_t} = R_{up\_t} - R_{release\_t} \quad \text{(S11)}$$

$$R_{blood\_t} = Q_t \times (C_a - CV_t) - PA_t \times CV_t + (PA_t \times C_{tissue\_t}) / P_t + R_{release\_t} - R_{up\_t} \quad \text{(S12)}$$

$$R_{tissue\_t} = PA_t \times CV_t - (PA_t \times C_{tissue\_t}) / P_t \quad \text{(S13)}$$

where R_{up_t} [mg/h] is the uptake rate of the NPs from the capillary blood to PCs in the organ *t*, K_{up_t} [per h] is the uptake rate parameter, A_{b_t} [mg] is the amount of the NPs in the capillary blood sub-compartment in the organ *t*, $R_{release\_t}$ [mg/h] is the release rate of the NPs from PCs to the capillary blood in the organ *t*, $K_{release\_t}$ [per h] is the release rate constant, A_{pc_t} [mg] is the amount of the NPs in PCs of the organ *t*, R_{pc_t} [mg/h] is the rate of changes in the mass of the NPs in the PCs sub-compartment in the organ *t*, R_{blood_t} [mg/h] is the rate of changes in the amount of the NPs in the capillary blood sub-compartment of the organ *t*, Q_t [L/h] is the blood flow to the organ *t*, C_a [mg/L] is the concentration of the NPs in the arterial blood, CV_t [mg/L] is the concentration of the NPs in the venous blood of the organ *t*, PA_t [L/h] is the permeability area cross product between the capillary blood and the tissue of the organ *t* (PA_t is approximated as the product of permeability coefficient between capillary blood and tissue [PAC_t : unitless] and regional blood flow [Q_t : L/h]), C_{tissue_t} [mg/L, μg/g or ng/g] is the concentration of the NPs in the tissue sub-compartment of the organ *t*, P_t [unitless] is the tissue:plasma distribution coefficient for the organ *t*, R_{tissue_t} [mg/h] is the rate of changes in the mass of the NPs in the tissue sub-compartment of the organ *t*.

The equations simulating the kinetics of 13nm PEG-coated AuNPs in the capillary blood, tissue, and PCs sub-compartments in the organ *t* are provided in the main text.

1.3. Elimination

Based on the experimental data from Cho et al. (2010), both the 13nm and 100nm PEG-coated AuNPs could be excreted via the bile and urine. Therefore, clearance terms were included in the liver and kidney compartments. For example, the equations describing the kinetics of the 13nm PEG-coated AuNPs in the liver, kidneys, bile, and urine are shown below:

$$R_{blood\_L} = Q_L \times (C_a - CV_L) + Q_S \times CV_S - PA_L \times CV_L + (PA_L \times C_{tissue\_L}) / P_L - R_{bile} \quad \text{(S14)}$$

$$R_{blood\_K} = Q_K \times (C_a - CV_K) - PA_K \times CV_K + (PA_K \times C_{tissue\_K}) / P_K - R_{urine} \quad \text{(S15)}$$

$$R_{bile} = K_{bile} \times CV_L \quad \text{(S16)}$$

$$R_{urine} = K_{urine} \times CV_K \quad \text{(S17)}$$

where R_{bile} [mg/h] is the rate of biliary excretion of the NPs, K_{bile} [L/h] is the biliary excretion rate constant of the NPs, R_{urine} [mg/h] is the rate of urinary excretion of the NPs, K_{urine} [L/h] is the urinary excretion rate constant of the NPs. The subscripts “K”, “L”, and “S” represent the kidneys, liver, and spleen, respectively. Detailed description of the other parameters refers to the Section 1.2.

2. Model parameterization

As mentioned in the main text, the PBPK model for the 13nm and 100nm AuNPs was calibrated with the 13nm and 100nm experimental datasets, respectively, from Cho et al. (2010). To this end, the physiological parameters for mice from Table S1 and the equations describing the pharmacokinetics of 13nm AuNPs in the main text and of 100nm AuNPs in Section 1 of the Supporting Material were utilized. The NP-dependent parameters were estimated by using both the Nelder-Mead maximum log likelihood estimation method in acslX and the manual approach. The Nelder-Mead computational-based approach was firstly done to estimate the approximated

values for the NP-dependent parameters (Lee et al., 2009; Li et al., 2014). Next, the manual approach was performed by adjusting the NP-dependent parameters iteratively until a visually optimal match between the PBPK model prediction and the in vivo data was obtained (Bachler et al., 2014).

The reasons for applying a visual fitting approach and its advantages compared to the computational-based approach in the development of PBPK models for NPs have been discussed previously (Mager et al., 2012; Bachler et al., 2014). In brief, firstly, due to the sparse nature of the data (data points available at 0.5h, 4h, 24h, and 168h) from Cho et al. (2010), it was not feasible to directly use computational-based approach for parameter estimation because of the great uncertainty in the concentration profile, especially during the period between 24h and 168h (Mager et al., 2012). Second, there were multiple NP-dependent parameters (e.g., uptake and release rate parameters, distribution and permeability coefficients for each organ) that were unknown and had to be estimated based on a single limited dataset, so the estimated values were of great standard deviations (Li et al., 2014). Third, by using the manual approach, some expertise-based considerations could be incorporated into the model calibration (Bachler et al., 2014), which made the parameter estimation more physiologically plausible.

All NP-dependent parameter values are provided in Table 1 in the main text. The step-by-step parameterization process is detailed below.

2.1. Selection of model structure and parameter starting values

The first step of model calibration was to decide a reasonable model structure and to collect starting values for parameter optimization. Regarding model structure, this study started with a simple traditional perfusion-limited model structure (Lee et al., 2009), and then added

complexity gradually, similar to the strategy utilized by Mager et al. (2012). Please refer to Table S3 for different model structures that have been tested in this study and the qualitative evaluation of each model. Briefly, a simple traditional perfusion-limited model (Model 1) based on Lee et al. (2009) failed to simulate the pharmacokinetics of 13nm or 100nm AuNPs. A simple traditional membrane-limited model (Model 2) similar to Li et al. (2012) could predict the pharmacokinetics of 100nm AuNPs, but not the 13nm AuNPs. Next, based on Lin et al. (2008), we used time-dependent tissue:plasma (or tissue:blood) distribution coefficients (Model 3 and Model 4) and found that this strategy did not work well for both sizes of AuNPs. Thereafter, we incorporated simulations of endocytosis of NPs from the blood into the liver and spleen using either a linear function (Li et al., 2014) or the Hill function into Models 1-2, generating Models 5-6 (with a linear function) and Models 7-8 (with the Hill function), which had acceptable predictions of the pharmacokinetics of 100nm AuNPs, but not the 13nm AuNPs. Next, we included codes describing endocytosis of NPs into the kidneys and lungs, added maximum uptake capacity for each organ based on Li et al. (2014), and decided to simulate the endocytosis of 13nm AuNPs from the tissue (100nm AuNPs from the blood), producing Model 9 and Model 10, which had good predictions for both sizes of AuNPs. Additional approaches, e.g., exclusion of the maximum uptake capacities or distribution coefficients, were also tried in order to simplify the model. It was found that the maximum uptake capacities could be excluded because with the dose used in Cho et al. (2010) the simulated endocytosis generally did not reach the maximum uptake capacities (Models 11 and 12). On the other hand, exclusion of distribution coefficients affected the pharmacokinetics of 100nm AuNPs minimally (Model 13), but it substantially altered the kinetics of 13nm AuNPs (Model 14), especially during the early time periods (within 20h after injection). Therefore, Models 11 and 12 were utilized as final model structures in this study (Figure 1).

In order to use relatively the most reliable parameter values, the previously validated parameter values from PBPK models for other NPs were utilized as starting values for further optimization in the present model as much as possible, including distribution coefficients and permeability coefficients from Li et al. (2014) and biliary and urinary excretion rate constants from Mager et al. (2012).

2.2. Distribution and permeability coefficients

Distribution coefficients for each organ (i.e., the liver, spleen, kidneys, and lungs) were optimized by visually fitting to the 13nm dataset from Cho et al. (2010). The 13nm dataset was used for estimating these parameters because there was a delay in the activation of endocytosis of the 13nm AuNPs, and thus the concentrations of 13nm AuNPs in these organs during early time periods after injection were mainly determined by the distribution coefficients. Consequently, the data points for 0.5h and 4h for each organ were used to estimate distribution coefficients for each compartment. In order to create the most parsimonious model, the distribution coefficients for the 13nm and 100nm AuNPs were set to be the same to minimize the number of estimated parameters, as done in Li et al. (2014).

Permeability coefficients from Li et al. (2014) were retained in the present model as much as possible with three exceptions. First, because of the different number of compartments between the present model and the model by Li et al. (2014), the rest-of-body compartment actually represented different tissues/organs in these two models. Hence, the permeability coefficient for the rest-of-body compartment in the present model had to be re-estimated, and it was estimated, together with the biliary and urinary excretion rate constants (explained below), by visually fitting to the plasma data from Cho et al. (2010). Second, the permeability coefficient for the brain was set to be 0 in Li et al. (2014) by assuming a highly efficient blood-brain barrier. However, because several studies have detected AuNPs in the brain of AuNP-exposed rodents [reviewed

by Lin et al. (2014)], we set the permeability coefficient for the brain the same as that for the rest-of-body compartment. Last, the permeability coefficient for the spleen in the 13nm PBPK model had to be increased to fit the measured concentrations of AuNPs in the spleen, especially the data point at day 7 after injection, which was substantially higher than those in any other organs. This was done because by using the permeability coefficient for the spleen from Li et al. (2014) our model consistently underestimated the measured concentration in the spleen on day 7. These results suggest that the high concentrations of AuNPs in the spleen were regulated not only by highly efficient endocytosis [i.e., the maximum uptake capacity for phagocytic cells per organ weight is more than 10-fold higher than any other organs (Li et al., 2014)], but also via high diffusion due to the large pore size of the capillary wall of the spleen [e.g., physiological upper limits of the capillary wall pore size in the spleen, liver, and kidneys are ~5 μm, ~280 nm, and ~15 nm, respectively (Bachler et al., 2013)]. As a result, the permeability coefficient for the spleen was higher than that in Li et al. (2014).

2.3. Biliary and urinary excretion rate constants

The biliary and urinary excretion rate constants, together with the permeability coefficient for the rest-of-body compartment, were estimated simultaneously using the Nelder-Mead method in acslX. The rationale of assigning the upper and lower bounds for optimizations was based on another NP PBPK model (Li et al., 2012). The derived approximated values were further optimized by visually fitting to measured concentrations in the plasma from Cho et al. (2010). This same approach was used for both 100nm and 13nm AuNPs.

2.4. Endocytosis-related parameters

In the context of PBPK models for NPs, the description of endocytosis using the Hill function is novel. Hence, there were no validated initial values for computational-based optimization of

endocytosis-related parameters. As a result, all these parameters (i.e., Hill coefficient [n_t], the time for reaching half maximum rate [K_{50_t}], the maximum uptake rate constant [$K_{\max\_t}$], and the release rate constant [$K_{release\_t}$] for the liver, spleen, kidneys, and lungs) had to be estimated via numerous iterative simulations by manual approach and some assumptions need to be made. For example, in the model for the 100nm AuNPs and for the liver compartment, after multiple iterative simulations, the Hill coefficient (n_t) and the time for half maximum rate (K_{50_t}) were set to be 0.1 and 24h, respectively. The Hill coefficient (n_t) determined the steepness of the Hill curve, i.e., the smaller the value was, the steeper the Hill curve was. Hence, this low value was assigned to fit the rapid increase in the concentrations of 100nm AuNPs in the liver after injection. The time for half maximum rate (K_{50_t}) determined when the uptake rate started to rise. This parameter was varied between 0.5h and 240h (the maximum simulation time in this study) and optimal fitting to the measured concentration in the liver was obtained when it was around 24h. After fixing these two parameters, the maximum uptake rate constant ($K_{\max\_t}$) and the release rate constant ($K_{release\_t}$) were estimated by visually fitting to measured concentrations in the liver from Cho et al. (2010). For the spleen, kidneys, and lungs, the Hill coefficient (n_t) and the time for half maximum rate (K_{50_t}) were set to be the same as those in the liver. Next, the maximum uptake rate constant and the release rate constant for each compartment were estimated by visually fitting to measured data for respective organs from Cho et al. (2010).

Similar parameterization strategy was applied to estimate the endocytosis-related parameters for the PBPK model of 13nm AuNPs. Interestingly, in line with our hypotheses, the PBPK model-predicted Hill coefficient and the time for half maximum rate in the liver and spleen were greater for the 13nm AuNPs than the 100nm AuNPs, which suggests a slower rate of

endocytosis for the 13nm AuNPs than for the 100nm AuNPs. Values for all NP-specific parameters are provided in Table 1 in the main text.

3. Supplementary discussion

3.1. The role of distribution coefficients in the PBPK modeling of nanoparticles

In the majority of existing NP PBPK models, the parameter tissue:plasma distribution coefficient (some researchers termed it partition coefficient) was included based on uneven distribution between tissue interstitial fluid and plasma potentially due to different biocorona compositions in these two locations (Lin et al., 2008; Lee et al., 2009; Li et al., 2012; Mager et al., 2012; Li et al., 2014). However, some investigators assumed that this parameter was not necessary in NP PBPK models and did not include it (Bachler et al., 2013, 2014). Thus, the importance of distribution coefficients in existing NP PBPK models is controversial. In the present study, simulation results from membrane-limited models with and without distribution coefficients were compared and the results showed that distribution coefficients affected the biodistribution of 100nm AuNPs minimally, but they substantially altered the kinetics of 13nm AuNPs, especially during the early time frame (≤4h; data not shown). These data are consistent with sensitivity analysis results where liver:plasma distribution coefficient had high influence on 24h liver AUC for 13nm AuNPs, but not on other selected dose metrics. The differential roles of distribution coefficient in the pharmacokinetics of different sizes of AuNPs are, in part, due to the time- and size-dependent endocytosis. Overall, our results highlight the importance of distribution coefficients in the early phase of pharmacokinetic process for small sizes of NPs. Therefore, this parameter should be included in the future NP PBPK models, especially for small size NPs.

3.2. The uncertainty of biliary and urinary excretion rate constants

The estimated biliary excretion rate constants are ~10-fold higher than the urinary clearance rate constants for both 13nm and 100nm AuNPs (Table 1). This trend is consistent with the 5-10

fold higher concentrations of 13nm AuNPs in the bile than in the urine (Cho et al., 2010). However, since neither the volume of the collected bile or urine, nor the % of injected dose in the bile or urine was provided, it was unfeasible to compare model simulated amount to measured concentrations. Thus, these data are not shown. Of note, the estimated biliary and urine excretion rate constants for 100nm AuNPs are greater than those for 13nm AuNPs. These results seem counter-intuitive as biliary and urinary excretion of NPs generally decreases with increasing sizes (Lin et al., 2014). This suggests that the biliary and urinary excretion rate constants might actually represent other mechanisms of clearance. Specifically, clearance of AuNPs from the blood depends on multiple mechanisms, including excretion via the bile and urine, endocytosis by cells in major organs (i.e., liver, spleen, kidneys, and lungs) and other organs (e.g., bone marrow), but the present model does not include endocytosis in other organs due to lack of experimental data. Hence, the estimated biliary and urinary excretion rate constants might in reality represent a combination of different clearance mechanisms. This lack of identifiability is a weakness of any pharmacokinetic model but can be rectified with additional data. This possibility requires further investigation using more discriminative study designs.

3.3 Preliminary simulation of long-term kinetics of PEG-coated AuNPs

In order to provide insights into long-term kinetic and PBPK modeling studies, the present model was applied to predict concentrations of Au in the liver and spleen of mice up to 6 months after intravenous injection with 0.85 mg/kg 13nm and 100nm PEG-coated AuNPs. Compared to experimental data (Cho et al., 2010), our model accurately predicted 13nm AuNPs concentration in the liver at 1 month, but over predicted it at 6 months post exposure; the concentrations of 13nm AuNPs in the spleen after 7 days were also over estimated by our model (Figure 6S). In addition, the model under predicted the concentrations of 100nm AuNPs in the liver and spleen at ≥1 months post exposure. Thus, the present model cannot be used to predict long-term kinetics of PEG-coated AuNPs. This is not unexpected because the model

was calibrated only with short-term kinetic data. These results suggest that other processes may be operative over these longer time frames. For example, intravenous injection to ≥0.85 mg/kg 13nm PEG-coated AuNPs caused acute inflammation and apoptosis in the liver (Cho et al., 2009), which may impair particle clearance systems, leading to persistent accumulation and/or overload. Additional long-term kinetic studies are needed to decipher mechanisms responsible for long-term kinetics and once these data become available, the present PBPK model may be refined to simulate long-term kinetics of AuNPs.

4. Supplementary tables

Table S1. Physiological parameters used in the PBPK model for PEG-coated gold nanoparticles in mice.

Parameter	Symbol	Value	Reference
Body weight (kg)	BW	0.02	Cho et al. (2010), Davies and Morris (1993)
Cardiac output (L/h/kg$^{0.75}$)	QCC	16.5	Brown et al. (1997)
Blood flow to organ (fraction of cardiac output, unitless)			
Liver	QLC	0.161	Brown et al. (1997)
Spleen	QSC	0.011	Lin et al. (2008), Davies and Morris (1993)
Kidneys	QKC	0.091	Brown et al. (1997)
Lungs	QLuC	1.00	Brown et al. (1997)
Brain	QBRC	0.033	Brown et al. (1997)
Rest of body	QrestC	0.704	Brown et al. (1997)
Organ volumes (fraction of body weight, unitless)			
Liver	VLC	0.055	Brown et al. (1997)
Spleen	VSC	0.005	Lin et al. (2008), Davies and Morris (1993)
Kidneys	VKC	0.017	Brown et al. (1997)
Lungs	VLuC	0.007	Brown et al. (1997)
Brain	VBRC	0.017	Brown et al. (1997)
Rest of body	VrestC	0.85	Brown et al. (1997)
Blood[a]	VBloodC	0.049	Brown et al. (1997)
Plasma	VPlasmaC	0.029	Davies and Morris (1993), Lin et al. (2011)
Volume fraction of blood in organs (unitless)			
Liver	BVL	0.31	Brown et al. (1997)
Spleen	BVS	0.17	Brown et al. (1997)
Kidneys	BVK	0.24	Brown et al. (1997)
Lungs	BVLu	0.50	Brown et al. (1997)
Brain	BVBR	0.03	Brown et al. (1997)
Rest of body[b]	BVrest	0.04	Brown et al. (1997)

[a] Arterial and venous blood account for 20% and 80% of the total blood, respectively (Li et al., 2014).
[b] Assumed to be the same as the value for the muscle (Brown et al., 1997).

Table S2. Pharmacokinetic studies used in the PBPK model calibration and evaluation.

Purpose	Dataset #	Size of PEG-coated AuNPs	Animal	Administration method and dosage	Selected time points	Selected organs/tissues	Detection method	References
Larger AuNPs								
Calibration	1	100nm	Mice	IV: 0.85 mg/kg	0.5, 4, 24 h, 7 days	Plasma, Liver, Spleen, Kidneys, Lungs	ICP-MS	Cho et al. (2010)
Evaluation	1	80nm, ^{111}In labeling	Mice, mice[#]	IV: 2 mg/kg[a]	0.5, 1, 2, 4, 8, 20, 28, 48 h	Plasma, Liver, Spleen	Gamma counter	Zhang et al. (2009)
Smaller AuNPs								
Calibration	1	13nm	Mice	IV: 0.85 mg/kg	0.5, 4, 24 h, 7 days	Plasma, Liver, Spleen, Kidneys, Lungs	ICP-MS	Cho et al. (2010)
Evaluation	1	13nm	Mice	IV: 0.85 mg/kg	5, 30 min, 4, 24 h, 7 days	Plasma, Liver, Spleen	ICP-MS	Cho et al. (2009)
	2	13nm	Mice	IV: 4.26 mg/kg	5, 30 min, 4, 24 h, 7 days	Plasma, Liver, Spleen	ICP-MS	Cho et al. (2009)
	3	20nm, ^{111}In labeling	Mice, mice[#]	IV: 2 mg/kg[a]	0.5, 1, 2, 4, 8, 20, 28, 48 h	Blood, Liver, Spleen, Kidneys	Gamma counter	Zhang et al. (2009)
	4	16nm	Mice[#]	IV: 5.88 mg/kg	24 h	Blood, Liver, Spleen, Kidneys, Lungs	ICP-MS	Liu et al. (2013)

Note: AuNPs: gold nanoparticles; PEG: polyethylene glycol; ICP-MS: inductively coupled plasma mass spectrometry. Mice[#]: tumor-bearing mice.

[a] The injection dose was set to be 2 mg/kg based on _ENREF_16Khlebtsov and Dykman (2011).

Table S3. Qualitative evaluation of different model structures that have been tested in the present study.

Model #	Model characteristics	13nm AuNPs	100nm AuNPs
1	A traditional perfusion-limited model	Poor	Poor
2	A traditional membrane-limited model	Poor	Good
3	A perfusion-limited model: distribution coefficients were set to be time-dependent	Poor	Poor
4	A membrane-limited model: distribution coefficients were set to be time-dependent	Poor	Poor
5	A perfusion-limited model: endocytosis of nanoparticles in the liver and spleen was described using a linear equation	Poor	Good
6	A membrane-limited model: endocytosis of nanoparticles in the liver and spleen was described using a linear equation	Poor	Good
7	A perfusion-limited model: endocytosis of nanoparticles in the liver and spleen was described using the Hill function	Poor	Good
8	A membrane-limited model: endocytosis of nanoparticles in the liver and spleen was described using the Hill function	Poor	Good
9	A membrane-limited model: endocytosis of nanoparticles in the liver, spleen, kidneys, and lungs was described using the Hill function; maximum uptake capacity for each organ was included; uptake of nanoparticles was from the blood	NA	Good
10	A membrane-limited model: endocytosis of nanoparticles in the liver, spleen, kidneys, and lungs was described using the Hill function; maximum uptake capacity for each organ was included; uptake of nanoparticles was from the tissue	Good	NA
11	A membrane-limited model: endocytosis of nanoparticles in the liver, spleen, kidneys, and lungs was described using the Hill function; uptake of nanoparticles was from the blood; maximum uptake capacity was excluded	NA	Good
12	A membrane-limited model: endocytosis of nanoparticles in the liver, spleen, kidneys, and lungs was described using the Hill function; uptake of nanoparticles was from the tissue; maximum uptake capacity was excluded	Good	NA
13	A membrane-limited model: endocytosis of nanoparticles in the liver, spleen, kidneys, and lungs was described using the Hill function; uptake of nanoparticles was from the blood; maximum uptake capacity was excluded; distribution coefficients were excluded	NA	Good
14	A membrane-limited model: endocytosis of nanoparticles in the liver, spleen, kidneys, and lungs was described using the Hill function; uptake of nanoparticles was from the tissue; maximum uptake capacity was excluded; distribution coefficients were excluded	Poor	NA

NA: not applicable; AuNPs: polyethylene glycol-coated gold nanoparticles.

Table S4. Comparison of highly sensitive physiological parameters among different species.

Parameter	Description	Mice[a]	Rats[a]	Beagle Dogs[a]	Mongrel Dogs[a]	Pigs[b]	Humans[a]
BW (kg)	Body weight	0.02	0.25	10	21	25	70
QCC ($L/h/Kg^{0.75}$)	Scaled cardiac output	16.5	18.74	22.94	17.96	11.055	12.89
VLC (unitless)	Liver volume fraction of BW	0.055	0.034	0.033	0.033	0.02	0.026
VplasmaC (unitless)	Plasma volume fraction of BW	0.029	0.04	0.048	0.048	0.040	0.044
BVL (unitless)	Blood volume fraction in liver	0.31	0.21	0.15	0.15	0.115	0.11

[a] Data are from Davies and Morris (1993) and Brown et al. (1997).
[b] Data are from Buur et al. (2005) and Upton (2008).

5. Supplementary figures

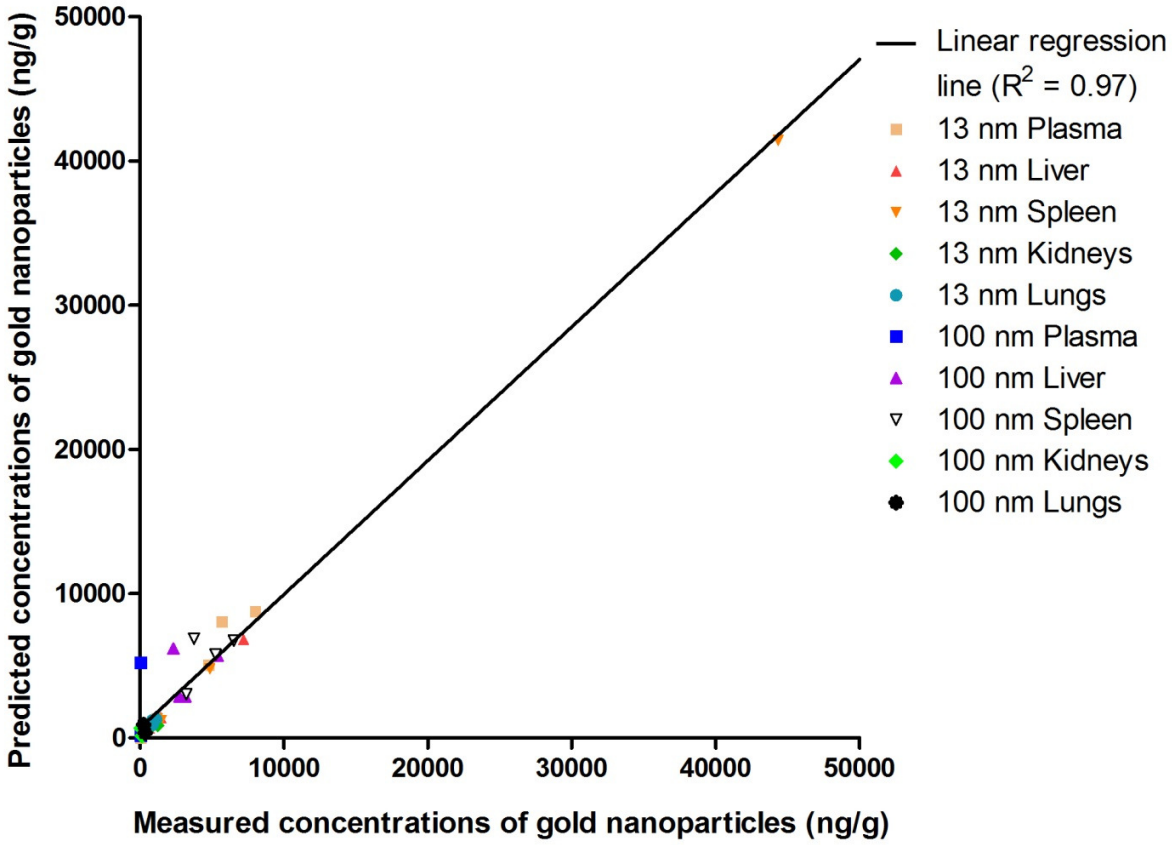

Figure S1. Goodness-of-fit plot of the linear regression analysis of model predictions and measured data for model calibration. Experimental data are from Cho et al. (2010). The linear regression coefficient (R^2) is 0.97.

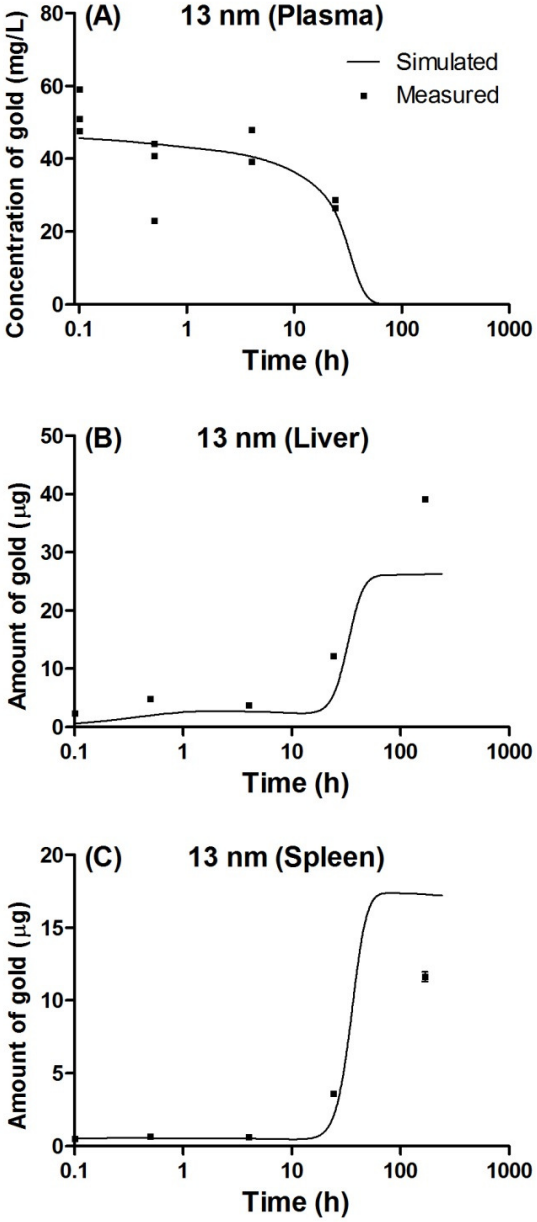

Figure S2. PBPK model evaluation results with the data from Cho et al. (2009). Model-predicted (solid lines) vs. measured (symbols) concentrations of gold in the plasma (A) or amounts of gold in the liver (B) and spleen (C) of healthy mice after iv injection with 4.26 mg/kg 13nm PEG-coated gold nanoparticles.

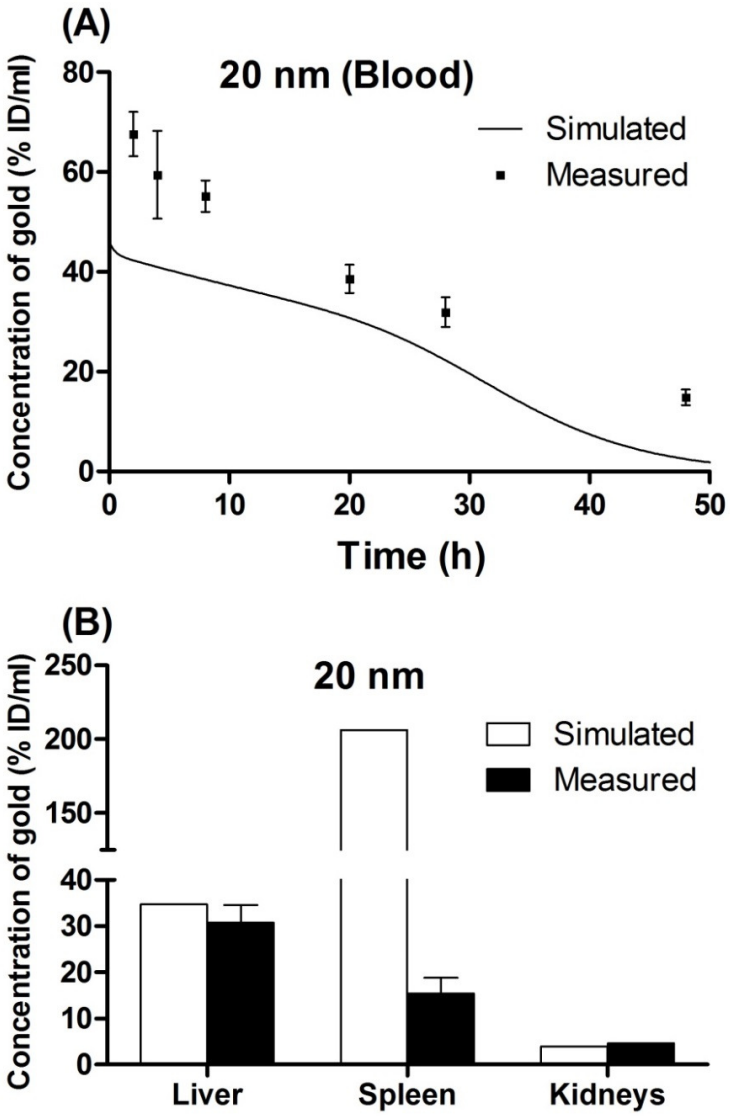

Figure S3. PBPK model evaluation results with the data from Zhang et al. (2009). (A) Comparison of model predictions (solid lines) and measured concentrations of gold in the blood of healthy mice after iv injection with 20nm PEG-coated gold nanoparticles. (B) Model predictions vs. measured concentrations of gold in the liver, spleen, and kidneys of tumor-bearing mice at 48h after iv injection with 20nm PEG-coated gold nanoparticles. ID: injection dose. The injection dose was set to be 2 mg/kg based on Khlebtsov and Dykman (2011).

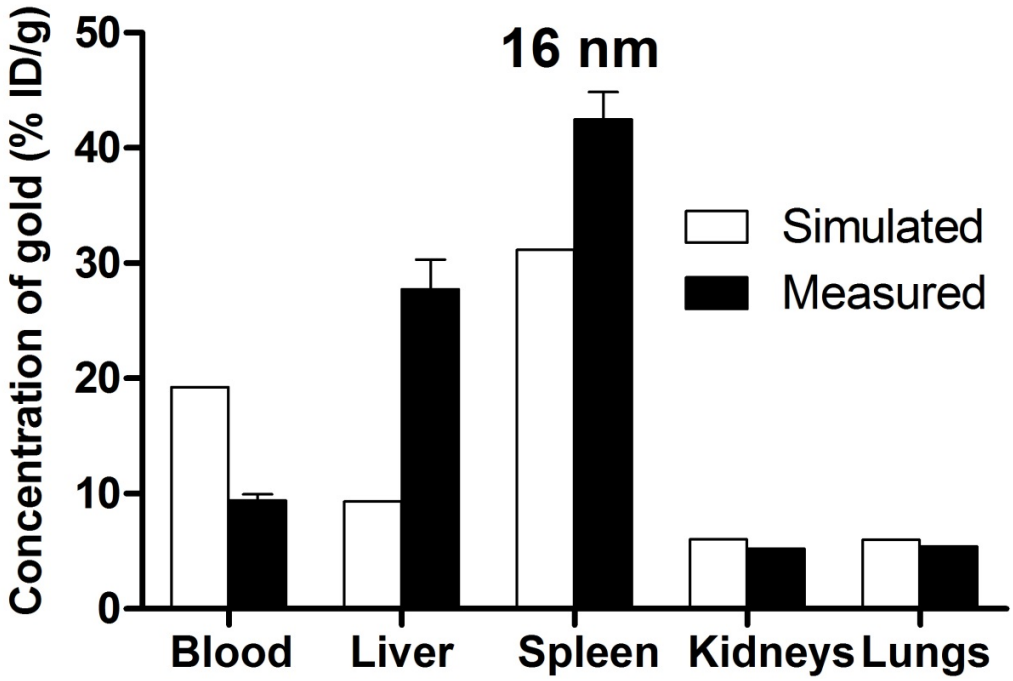

Figure S4. PBPK model evaluation results with the data from _ENREF_13Liu et al. (2013). Data represent simulated and measured concentrations (mean ± SD) of gold in the blood or tissues of tumor-bearing mice at 24h after iv injection with 5.88 mg/kg 16nm PEG-coated gold nanoparticles. ID: injection dose.

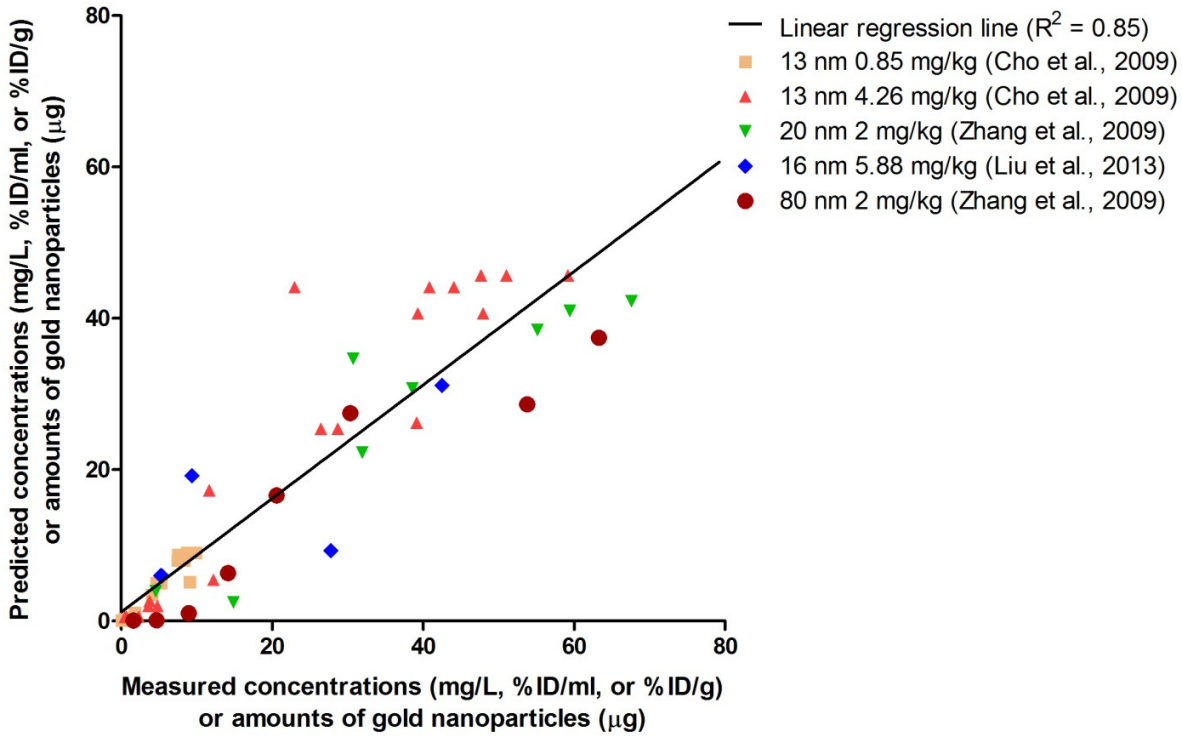

Figure S5. Goodness-of-fit plot of the linear regression analysis of model predictions and measured data for model evaluation. Experimental data are from Cho et al. (2009), Zhang et al. (2009), and Liu et al. (2013). The linear regression coefficient (R^2) is 0.85.

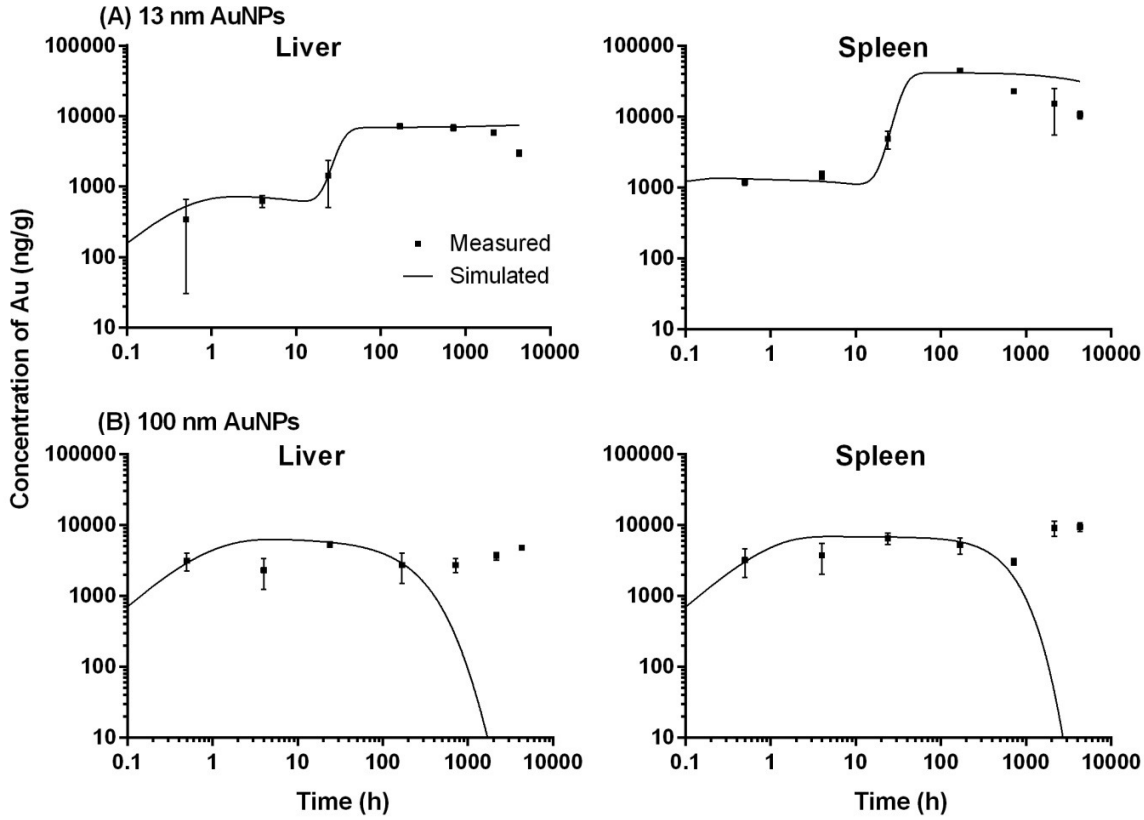

Figure S6. Preliminary simulation results of long-term kinetics of PEG-coated gold nanoparticles (AuNPs). Comparison of PBPK model predictions (solid lines) and measured concentrations in the liver and spleen of mice after iv injection with 0.85 mg/kg 13nm (A) or 100nm (B) PEG-coated AuNPs. Experimental data are from Cho et al. (2010).

6. References:

Bachler G, von Goetz N, Hungerbuhler K. 2013. A physiologically based pharmacokinetic model for ionic silver and silver nanoparticles. Int J Nanomedicine 8:3365-82.

Bachler G, von Goetz N, Hungerbuhler K. 2014. Using physiologically based pharmacokinetic (PBPK) modeling for dietary risk assessment of titanium dioxide (TiO) nanoparticles. Nanotoxicology 1-8.

Brown RP, Delp MD, Lindstedt SL, Rhomberg LR, Beliles RP. 1997. Physiological parameter values for physiologically based pharmacokinetic models. Toxicol Ind Health 13:407-84.

Buur JL, Baynes RE, Craigmill AL, Riviere JE. 2005. Development of a physiologic-based pharmacokinetic model for estimating sulfamethazine concentrations in swine and application to prediction of violative residues in edible tissues. Am J Vet Res 66:1686-93.

Cho WS, Cho M, Jeong J, Choi M, Cho HY, Han BS, et al. 2009. Acute toxicity and pharmacokinetics of 13 nm-sized PEG-coated gold nanoparticles. Toxicol Appl Pharmacol 236:16-24.

Cho WS, Cho M, Jeong J, Choi M, Han BS, Shin HS, et al. 2010. Size-dependent tissue kinetics of PEG-coated gold nanoparticles. Toxicol Appl Pharmacol 245:116-23.

Davies B, Morris T. 1993. Physiological parameters in laboratory animals and humans. Pharm Res 10:1093-5.

Khlebtsov N, Dykman L. 2011. Biodistribution and toxicity of engineered gold nanoparticles: a review of in vitro and in vivo studies. Chem Soc Rev 40:1647-71.

Lee HA, Leavens TL, Mason SE, Monteiro-Riviere NA, Riviere JE. 2009. Comparison of quantum dot biodistribution with a blood-flow-limited physiologically based pharmacokinetic model. Nano Lett 9:794-9.

Li D, Johanson G, Emond C, Carlander U, Philbert M, Jolliet O. 2014. Physiologically based pharmacokinetic modeling of polyethylene glycol-coated polyacrylamide nanoparticles in rats. Nanotoxicology 8:128-37.

Li M, Panagi Z, Avgoustakis K, Reineke J. 2012. Physiologically based pharmacokinetic modeling of PLGA nanoparticles with varied mPEG content. Int J Nanomedicine 7:1345-56.

Lin P, Chen JW, Chang LW, Wu JP, Redding L, Chang H, et al. 2008. Computational and ultrastructural toxicology of a nanoparticle, Quantum Dot 705, in mice. Environ Sci Technol 42:6264-70.

Lin Z, Fisher JW, Ross MK, Filipov NM. 2011. A physiologically based pharmacokinetic model for atrazine and its main metabolites in the adult male C57BL/6 mouse. Toxicol Appl Pharmacol 251:16-31.

Lin Z, Monteiro-Riviere NA, Riviere JE. 2014. Pharmacokinetics of metallic nanoparticles. Wiley Interdiscip Rev Nanomed Nanobiotechnol (In press).

Liu X, Huang N, Wang H, Li H, Jin Q, Ji J. 2013. The effect of ligand composition on the in vivo fate of multidentate poly(ethylene glycol) modified gold nanoparticles. Biomaterials 34:8370-81.

Mager DE, Mody V, Xu C, Forrest A, Lesniak WG, Nigavekar SS, et al. 2012. Physiologically based pharmacokinetic model for composite nanodevices: effect of charge and size on in vivo disposition. Pharm Res 29:2534-42.

Upton RN. 2008. Organ weights and blood flows of sheep and pig for physiological pharmacokinetic modelling. J Pharmacol Toxicol Methods 58:198-205.

Zhang G, Yang Z, Lu W, Zhang R, Huang Q, Tian M, et al. 2009. Influence of anchoring ligands and particle size on the colloidal stability and in vivo biodistribution of polyethylene glycol-coated gold nanoparticles in tumor-xenografted mice. Biomaterials 30:1928-36.

7. PBPK model code for the 13nm PEG-coated gold nanoparticles

```
PROGRAM
        INITIAL
                ! code that is executed once at the beginning of a simulation run goes here
! Blood flow rate (Fraction of cardiac output)
CONSTANT QCC = 16.5 ! Cardiac output (L/h/kg^0.75) (Brown et al., 1997)
CONSTANT QLC = 0.161 ! Fraction of blood flow to liver (Brown et al., 1997, Table 23)
CONSTANT QBRC = 0.033 ! Fraction of blood flow to brain (Brown et al., 1997, Table 23)
CONSTANT QKC = 0.091 ! Fraction of blood flow to kidneys (Brown et al., 1997, Table 23)
CONSTANT QSC = 0.011 ! Fraction of blood flow to spleen (Lin et al., 2008; Davies and Morris,
1993)

! Tissue volumes (Fraction of body weight)
CONSTANT BW = 0.02 ! Body weight (kg) (Cho et al., 2009; 2010)
CONSTANT VLC = 0.055 ! Liver (Brown et al., 1997, Table 21)
CONSTANT VBRC = 0.017 ! Brain (Brown et al., 1997, Table 21)
CONSTANT VKC = 0.017 ! Kidneys (Brown et al., 1997, Table 21)
CONSTANT VSC = 0.005 ! Spleen (Lin et al., 2008; Davies and Morris, 1993)
CONSTANT VLuC = 0.007 ! Lungs (Brown et al., 1997, Table 21)
CONSTANT VBloodC = 0.049 ! Blood (Brown et al., 1997, Table 21)
CONSTANT VPlasmaC = 0.029 ! Plasma (Davies and Morris, 1993; Lin et al., 2011)

! Blood volume fraction in organs and tissues (percentage of tissues)
CONSTANT BVL = 0.31 ! Liver (Brown et al., 1997; Table 30)
CONSTANT BVBR = 0.03 ! Brain (Brown et al., 1997; Table 30)
CONSTANT BVK = 0.24 ! Kidneys (Brown et al., 1997; Table 30)
CONSTANT BVS = 0.17 ! Spleen (Brown et al., 1997; Table 30)
CONSTANT BVLu = 0.50 ! Lungs (Brown et al., 1997; Table 30)
CONSTANT BVrest = 0.04 ! Rest of body (Brown et al., 1997; Table 30, assume the same as
the muscle)

! Distribution coefficients (PC), unitless (Based on Li et al., 2014)
CONSTANT PL = 0.08!Liver:plasma PC
CONSTANT PBR = 0.15!Brain:plasma PC
CONSTANT PK = 0.15!Kidneys:plasma PC
CONSTANT PS = 0.15!Spleen:plasma PC
CONSTANT PLu =0.15!Lungs:plasma PC
CONSTANT Prest = 0.15!Rest of body:plasma PC

! Diffusion limitation coefficient constants, unitless (Based on Li et al., 2014)
CONSTANT PALC = 0.001!Permeability coefficient between blood and liver
CONSTANT PABRC = 0.000001!Permeability coefficient between blood and brain
CONSTANT PAKC = 0.001!Permeability coefficient between blood and kidneys
CONSTANT PASC = 0.03!Permeability coefficient between blood and spleen
CONSTANT PALuC = 0.001!Permeability coefficient between blood and lungs
CONSTANT PArestC = 0.000001!Permeability coefficient between blood and rest of body

! Endocytosis-related parameters; RES represent phagocytic cells; L, S, K, and Lu represent
liver, spleen, kidneys, and lungs, respectively.
CONSTANT KLRESrelease = 0.001
```

```
CONSTANT KLRESmax = 20
CONSTANT KLRES50 =48
CONSTANT KLRESn = 5

CONSTANT KSRESrelease = 0.001
CONSTANT KSRESmax = 40
CONSTANT KSRES50 = 48
CONSTANT KSRESn = 5

CONSTANT KKRESrelease = 0.0004
CONSTANT KKRESmax = 0.075
CONSTANT KKRES50 = 24
CONSTANT KKRESn = 5

CONSTANT KLuRESrelease = 0.003
CONSTANT KLuRESmax =0.075
CONSTANT KLuRES50 = 24
CONSTANT KLuRESn = 5

! Biliary excretion
!CONSTANT KbileC = 0.0027575 ! Biliary clearance (L/hr/kg^0.75)
CONSTANT Kbile = 0.00003!Biliary clearance (L/hr)
! Urine excretion
!CONSTANT KurineC = 0.001 ! Urine clearance (L/hr/kg^0.75)
CONSTANT Kurine = 0.000003!Urine clearance (L/hr)

! IV dosing
CONSTANT Timeiv = 0.005 ! IV infusion time (h), set, approximately 15-20 seconds, on
average 18 sec
CONSTANT PDOSEiv = 0.85 ! mg/kg

END ! INITIAL

DYNAMIC

ALGORITHM IALG = 2
NSTEPS    NSTP = 10
MAXTERVAL MAXT = 1.0e9
MINTERVAL MINT = 1.0e-9
CINTERVAL CINT = 0.1

DERIVATIVE
! code for calculating the derivative goes here
! Scaled parameters
! Cardiac output and regional blood blow (L/h)
QC = QCC*BW**0.75 ! Cardiac output
QL = QC*QLC ! Blood flow to liver
QBR = QC*QBRC ! Blood flow to brain
QK = QC*QKC ! Blood flow to kidney
QS = QC*QSC ! Blood flow to spleen
Qrest = QC-QL-QBR-QK-QS! Blood flow to rest of body
```

```
Qbal = QC-QL-QBR-QK-QS-Qrest ! Blood flow balance equation

! Tissue volumes (L)
VL = BW*VLC ! Liver
VBR = BW*VBRC ! Brain
VK = BW*VKC ! Kidney
VS = BW*VSC ! Spleen
VLu = BW*VLuC ! Lungs
VBlood = BW*VBloodC
VPlasma = BW*VPlasmaC
Vrest = BW-VL-VBR-VK-VS-VLu-VPlasma
Vbal = BW-VL-VBR-VK-VS-VLu-VPlasma-Vrest
VLb = VL*BVL ! Weight/volume of capillary blood in liver compartment
VLt = VL-VLb ! Weight/volume of tissue in liver compartment
VBRb = VBR*BVBR ! Weight/volume of capillary blood in brain compartment
VBRt = VBR-VBRb ! Weight/volume of tissue in brain compartment
VKb = VK*BVK ! Weight/volume of capillary blood in kidney compartment
VKt = VK-VKb ! Weight/volume of tissue in kidney compartment
VSb = VS*BVS ! Weight/volume of capillary blood in spleen compartment
VSt = VS-VSb ! Weight/volume of tissue in spleen compartment
VLub = VLu*BVLu ! Weight/volume of capillary blood in Lung compartment
VLut = VLu-VLub ! Weight/volume of tissue in Lung compartment
Vrestb = Vrest*BVrest ! Weight/volume of capillary blood in rest of body compartment
Vrestt = Vrest-Vrestb ! Weight/volume of tissue in rest of body compartment

! Permeability coefficient-surface area cross-product
PAL = PALC*QL
PABR = PABRC*QBR
PAK = PAKC*QK
PAS = PASC*QS
PALu = PALuC*QC
PArest = PArestC*Qrest

KLRESUP = ((KLRESmax*T^KLRESn)/(KLRES50^KLRESn+T^KLRESn))
KSRESUP = ((KSRESmax*T^KSRESn)/(KSRES50^KSRESn+T^KSRESn))
KKRESUP = ((KKRESmax*T^KKRESn)/(KKRES50^KKRESn+T^KKRESn))
KLuRESUP = ((KLuRESmax*T^KLuRESn)/(KLuRES50^KLuRESn+T^KLuRESn))

! Dosing
DOSEiv = PDOSEiv*BW ! mg
IVR = DOSEiv/Timeiv ! mg/h
RIV = IVR*(1.-step(Timeiv))
AIV = Integ(RIV, 0.0)

! Elimination
!Kbile = KbileC*BW**0.75 ! L/h
!Kurine = KurineC*BW**0.75 ! L/h

!! Blood compartment: arterial and venous blood account for 20% and 80% of the total blood, respectively (Li et al., 2014)
! CA = Arterial blood concentration (mg/L or ug/ml)
```

```
RA = QC*CVLu - QC*CA
AA = Integ(RA, 0.0)
!CA = AA/(VBlood*0.2)
CA = AA/(VPlasma*0.2)
AUCCA = Integ(CA,0.0)
CA1000 = CA*1000 ! ng/g, ng/ml, ug/L
AUCCA1000 = Integ(CA1000,0.0)

! CV = Venous blood concentration (mg/L or ug/ml)
RV = QL*CVL + QBR*CVBR + QK*CVK + Qrest*CVrest + RIV - QC*CV !
AV = Integ(RV, 0.0)
!CV = AV/(VBlood*0.8)
CV = AV/(VPlasma*0.8)
APlasma = AA+AV
APlasmaperc = 100*(APlasma/Doseiv)/(VPlasma*1000)
!Abloodperc = 100*(ABlood/Doseiv)/(VBlood*1000)

!! Lung compartment
! Membrane-limited model
RLub = QC*(CV-CVLu) - PALu*CVLu + (PALu*CLut)/PLu
ALub = Integ(RLub,0.0)
CVLu = ALub/VLub

RLut = PALu*CVLu - (PALu*CLut)/PLu - KLuRESUP*ALut + KLuRESrelease*ALuRES
ALut = Integ(RLut,0.0)
CLut = ALut/VLut
ALutotal = ALub+ALut
CLu = ALutotal/VLu
CLu1000 = CLu*1000 ! ng/g, ng/ml, ug/L

RLuRES = KLuRESUP*ALut-KLuRESrelease*ALuRES
RLuRESUP = KLuRESUP*ALut!
RLuRESrelease = KLuRESrelease*ALuRES
ALuRES = INTEG(RLuRES,0.0)
CLung = (ALutotal+ALuRES)/VLu
CLungtissue = (ALut+ALuRES)/VLut
Clungtissue1000 = 1000*(ALut+ALuRES)/VLut
Alungtissue1000 = 1000*(ALut+ALuRES)
Alung1000 = 1000*(ALut+ALub+ALuRES)
Alungblood1000 = 1000*ALub
CLung1000 = CLung*1000

ALungtissue = ALut+ALuRES
ALungtissueperc = 100*(ALungtissue/Doseiv)/(VLut*1000)

!! Brain compartment
! Membrane-limited model
RBRb = QBR*(CA-CVBR) - PABR*CVBR + (PABR*CBRt)/PBR
ABRb = Integ(RBRb,0.0)
CVBR = ABRb/VBRb
```

```
RBRt = PABR*CVBR - (PABR*CBRt)/PBR
ABRt = Integ(RBRt,0.0)
CBRt = ABRt/VBRt
ABRtotal = ABRb+ABRt
CBR = ABRtotal/VBR

!! Rest of body compartment
! Membrane-limited model
Rrestb = Qrest*(CA-CVrest) - PArest*CVrest + (PArest*Crestt)/Prest
Arestb = Integ(Rrestb,0.0)
CVrest = Arestb/Vrestb

Rrestt = PArest*CVrest - (PArest*Crestt)/Prest
Arestt = Integ(Rrestt,0.0)
Crestt = Arestt/Vrestt
Aresttotal = Arestb+Arestt
Crest = Aresttotal/Vrest

!! Kidney compartment
! Membrane-limited model
RKb = QK*(CA-CVK) - PAK*CVK + (PAK*CKt)/PK - Rurine
AKb = Integ(RKb,0.0)
CVK = AKb/VKb

RKt = PAK*CVK - (PAK*CKt)/PK - KKRESUP*AKt + KKRESrelease*AKRES
AKt = Integ(RKt,0.0)
CKt = AKt/VKt
AKtotal = AKb+AKt
CK = AKtotal/VK
CK1000 = CK*1000 ! ng/g, ng/ml, ug/L

! Urinary excretion
Rurine = Kurine*CVK ! mg/h
Aurine = Integ(Rurine,0.0)

RKRES = KKRESUP*AKt-KKRESrelease*AKRES
RKRESUP = KKRESUP*AKt!
RKRESrelease = KKRESrelease*AKRES
AKRES = INTEG(RKRES,0.0)
CKidney = (AKtotal+AKRES)/VK
CKidneytissue1000 = 1000*(AKt+AKRES)/VKt
AKidneytissue1000 = 1000*(AKt+AKRES)
AKidney1000 = 1000*(AKt+AKb+AKRES)
AKidneyblood1000 = 1000*AKb
CKidney1000 = CKidney*1000

AKidneytissue = AKt+AKRES
AKidneytissueperc = 100*(AKidneytissue/Doseiv)/(VKt*1000)

!! Spleen compartment
! Membrane-limited model
```

```
RSb = QS*(CA-CVS) - PAS*CVS + (PAS*CSt)/PS
ASb = Integ(RSb,0.0)
CVS = ASb/VSb

RSt = PAS*CVS - (PAS*CSt)/PS - KSRESUP*ASt + KSRESrelease*ASRES
ASt = Integ(RSt,0.0)
CSt = ASt/VSt
AStotal = ASb+ASt
CS = AStotal/VS
CS1000 = CS*1000 ! ng/g, ng/ml, ug/L

RSRES = KSRESUP*ASt-KSRESrelease*ASRES
RSRESUP = KSRESUP*ASt!
RSRESrelease = KSRESrelease*ASRES
ASRES = INTEG(RSRES,0.0)
CSpleen = (AStotal+ASRES)/VS
CSpleentissue1000 = 1000*(ASt+ASRES)/VSt
AUCCSpleentissue1000 = Integ(CSpleentissue1000,0.0)
ASpleentissue1000 = 1000*(ASt+ASRES)
ASpleen1000 = 1000*(ASt+ASb+ASRES)
ASpleenblood1000 = 1000*ASb
CSpleen1000 = CSpleen*1000
ASpleentissue = ASt+ASRES
ASpleentissueperc = 100*(ASpleentissue/Doseiv)/(VSt*1000)

!! Liver compartment

! Membrane-limited model
RLb = QL*(CA-CVL) + QS*CVS - PAL*CVL + (PAL*CLt)/PL - Rbile
ALb = Integ(RLb,0.0)
CVL = ALb/VLb

RLt = PAL*CVL - (PAL*CLt)/PL - KLRESUP*ALt + KLRESrelease*ALRES
ALt = Integ(RLt,0.0)
CLt = ALt/VLt
ALtotal = ALb+ALt
CL = ALtotal/VL
CL1000 = CL*1000 ! ng/g, ng/ml, ug/L

RLRES = KLRESUP*ALt-KLRESrelease*ALRES
RLRESUP = KLRESUP*ALt!
RLRESrelease = KLRESrelease*ALRES
ALRES = INTEG(RLRES,0.0)
CLiver = (ALtotal+ALRES)/VL
CLivertissue1000 = 1000*(ALt+ALRES)/VLt
AUCClivertissue1000 = Integ(Clivertissue1000,0.0)
CLivertissue = (ALt+ALRES)/VLt
ALivertissue1000 = 1000*(ALt+ALRES)
ALiver1000 = 1000*(ALt+ALb+ALRES)
ALiverblood1000 = 1000*ALb
CLiver1000 = CLiver*1000
```

```
ALivertissue = ALt+ALRES
ALivertissueperc = 100*(ALivertissue/Doseiv)/(VLt*1000)

! Biliary excretion
Rbile = Kbile*CVL ! mg/h
Abile = Integ(Rbile,0.0)

! Mass balance
Tmass = AA + AV + ALtotal + ABRtotal + AKtotal + ALutotal + Aresttotal + AStotal + Abile +
Aurine + ALRES + ASRES + AKRES + ALuRES
Bal = AIV-Tmass

END ! DERIVATIVE

                ! Add discrete events here as needed
                !  DISCRETE
                !  END

                ! code that is executed once at each communication interval goes here

                CONSTANT TSTOP = 240.0
                TERMT (T .GE. TSTOP, 'checked on communication interval: REACHED
TSTOP')

        END ! DYNAMIC

        TERMINAL
                ! code that is executed once at the end of a simulation run goes here
        END ! TERMINAL

END ! PROGRAM
```